FLOODSTAND
FP7-RTD- 218532

Integrated Flooding Control and Standard for Stability and Crises Management

FLOODSTAND-deliverable:

IMPACT OF SHIP DYNAMICS IN FLOODING SIMULATION

Authors	Teemu Manderbacka
Organisations	AALTO
Revision	1.1
Deliverable No.	D3.2
Date	3 October 2011

Document identification sheet

FLOODSTAND	**Integrated Flooding Control and Standard for Stability and Crises Management**	FP7-RTD- 218532

Title: Impact of the Ship Dynamics in the Flooding Simulation	**Other report identifications:**
Investigating partners: AALTO, NAPA, MARIN **Authors:** Teemu Manderbacka **Reviewed by**: Jerzy Matusiak, Pekka Ruponen	
[ ] **Outline** [ ] **Draft** [x] **Final** **Version number:** 1.1 **Revision date**: 3 October 2011 **Next version due:** **Number of pages**: 24	[x] **A deliverable** [ ] **Part of a deliverable** [ ] **Cover document for a part of a deliverable** [ ] **Deliverable cover document** [ ] **Other** **Deliverable number**: D3.2 **Work Package**: WP3 **Deliverable due at month**: 26 (SC: => 28)
Accessibility: [x] **Public** [ ] **Restricted** [ ] **Confidential (consortium only)** [ ] **Internal (accessibility defined for the final version)**	**Available from**: http://floodstand.aalto.fi **Distributed to**: **Disclosees when restricted:** **Comments:**

Abstract:
The roll motions of a modern passenger cruise vessel are studied in two different damage cases. NAPA Flooding simulation tool is applied for the study of the floodwater progression in a calm water condition. The impact of ship dynamics are studied in damage case by applying the floodwater to a seakeeping and manoeuvring code LAIDYN. The lumped mass concept for floodwater modelling is adopted and described. The impact of the irregular waves to the roll motion is studied. With the applied method the transient and the wave induced ship motions are seen to occur in average around the quasi-static predicted heel angle.

Acknowledgements
The research leading to these results has received funding from the European Union's Seventh Framework Programme (FP7/2007-2013) under grant agreement n° 218532. The financial support is gratefully appreciated. The contribution of Pekka Ruponen and Napa Ltd. is greatly valued.

CONTENTS

1 EXECUTIVE SUMMARY

The objective of the WP3 Task 3.2 was to study the impact of the sea state to the reliability of the system of flood sensors and simulation tools for predicting of ship motions. In order to account for the sea state in the flooding simulation a dynamic model of sea keeping simulations must be integrated with the flooding simulations. The LAIDYN code developed at the Aalto University for the sea keeping and manoeuvring simulations and the NAPA flooding simulation codes are applied to study the damaged ship motions and flooding at the calm sea and wave conditions.

Case studies for a damaged passenger cruise ship design, a concept ship of 63.000 GT with length of 238 meters, were performed. Two different damage scenarios were simulated in irregular sea conditions. First damage scenario is a damage of two rooms on the side of the ship. In addition third room is flooded through a cross flooding duct. The breach size allows fast and asymmetric flooding which results in a pronounced transient roll motion.

The second damage case is a raking damage over three compartments. Breach size is smaller and flooding is slower than in the first damage scenario. Ship design, in this damage case, was intentionally changed to have poorer transversal damage stability. In the second damage case the transient motions are not that important but the damage and divisions of the flooded rooms result in larger heel angle.

The progression of the flooding was simulated in the calm water conditions using quasi-static simulation method. The roll motions were simulated by the dynamic simulation method, which could account for the transient ship motions due to flooding and the wave induced motions. Floodwater mass from the quasi-static simulation is applied to the dynamic simulation code. Dynamic ship motions both in the damage and intact case were then simulated in the presence of irregular beam seas. Exactly the same sets of irregular waves were applied to the intact and damaged cases.

Comparison of the roll motion between the intact and damaged cases in the irregular waves shows that the damaged ship rolls largely around the heel angle predicted by the quasi-static simulation in the calm water. In the applied model the floodwater volumes are not affected by the ship motions and the floodwater free surface remains horizontal. Thus some important phenomena of the floodwater behaviour are omitted for the sake of simplicity. The dynamic behaviour of the floodwater depends on many factors like detailed geometry of the flooded room and its permeability. More detailed modelling requires specific information on the obstacles in the rooms which is often not even available.

If the flooding is to be predicted with some sensor system the transient and wave induced motions should be filtered out from the sensor output. Simulations of ship motions with the described model of given amounts of floodwater clearly show that the average roll angle is of same magnitude than the quasi-static result in calm water. This gives a possibility to predict the overall flooding by using moving average over a time period longer than the ship natural roll period to smoothen the output. The dynamic simulation predicted roll angle processed by moving average, results in a quite close accordance with the quasi-static heel angle. Yet again the use of the floodwater volumes from the quasi-static simulation is a strong limitation of the applied dynamic simulation model and does not allow a real interaction of the ship and floodwater motions. The importance of this limitation should be studied further on.

2 INTRODUCTION

2.1 Background

The safety of large number of passengers that a modern passenger cruise vessel can accommodate is of utmost importance. In case of an accident resulting in the loss of watertight integrity of the ship and consequent flooding, the available options to ensure the safety of the passengers are the transportation of the ship to the port or evacuation. The feasibility of these options depends greatly on the residual stability of the ship after the damage. Onboard tools for fast assessment of the damage ship residual stability would be of great aid. Real time assessment of the available time for rescue operations requires either high performance computation tools or simplified assessment methods. Floodwater modeling in the room with various obstacles is cumbersome and sometimes even impossible due to the lack of information of the obstacle geometries. The simplifying assumption of clear flooded rooms would only be true in case of a ro-pax car deck without the cars, trucks and trailers. Most rooms in cruise vessels have equipment or other obstacles disturbing the floodwater flow.

2.2 Task definition

This task will focus on studying the impact of the sea environment on the reliability of the system of flood sensors and simulation tools for predicting of ship response. Flooding simulations for a damaged ship in calm water and in various sea states will be performed. The motions will be evaluated for different sea states.

2.3 Previous work

Tools to simulate the progressive flooding in a complex compartment spaces like the ones of passenger ships have been developed successfully by *Ruponen (2007)* using quasi-static simulation of motions. Damaged ship simulations developed for ro-ro/passenger ferries address to the dynamics of the floodwater and its effects to the ship motions *(Papanikolaou (2008), Jasionowski (2001), Santos and Soares (2008), de Kat (2000))* with a few flooded compartments mainly car deck or engine room.

3 SIMULATION METHOD

Flooding through a damage opening is simulated in calm water conditions with the NAPA Flooding Simulation tool. The amounts of flooded water in each room are given as an input to the dynamic ship motion simulation performed with LAIDYN. The floodwater free surface is assumed to remain horizontal at each time step of the simulations. This assumption is adopted partly due the simplicity in the simulations. Floodwater dynamic behaviour in the rooms where the engine block and related equipment are located is complicated to simulate and requires detailed computational time consuming discrete modelling. A model of the floodwater free surface being fixed to the quasi-static heel angle is described by *Manderbacka et al (2011)* and the results with horizontal free surface model are compared.

3.1 Flooding simulation

Simulation of the progressive flooding was performed with the NAPA Flooding Simulation tool, the method used is described by *Ruponen (2006, 2007).* Progression of the flooding is calculated in calm water. Pressure difference between both sides of the openings is caused by the difference in the height of the water level between the sides. Full ventilation is assumed in all flooded rooms. Water inside the rooms is assumed to remain horizontal. The flow velocity at the opening is calculated from the pressure difference using the Bernoulli equation. Static equilibrium position of the ship at each time step is calculated. Ship motions are assumed not to have an impact to the flooding at this stage.

3.2 Simulation of ship motions

Ship dynamics code LAIDYN is developed for intact ship seakeeping and manoeuvring simulations, hence the effect of the flooded mass had to be implemented to the code. The LAIDYN manages large non-linear ship motions and wave forces. The restoring Froude-Krylov forces are integrated over instantaneous wetted ship hull. The methods implemented in the intact ship LAIDYN code are described in more detail in *Matusiak (2003, 2007 and 2010).* Sloshing of the floodwater is assumed not to be important in relatively small spaces of the cruise ship. The floodwater at each room is taken into account as a lumped mass concentrated to its centre of buoyancy. The implementation of the lumped mass method to the LAIDYN is described in *Manderbacka et al (2011).* The equations of motion are applied to solve the ship motions. The equations are written in the ship fixed coordinate system for the ship and for each lumped mass. Equations of motion for the ship (eqs. 1 and 2) and lumped mass (3) are

$$m[\dot{\mathbf{u}} + \boldsymbol{\omega} \times \mathbf{u}] = \mathbf{f}_{ext} + m\mathbf{g} - \mathbf{f}_i \qquad (1)$$

$$\mathbf{I}\dot{\boldsymbol{\omega}} + \boldsymbol{\omega} \times \mathbf{I}\boldsymbol{\omega} = \mathbf{m}_{ext} - \mathbf{r}_i \times \mathbf{f}_i \qquad (2)$$

$$\begin{aligned} m_i[\dot{\mathbf{u}} + \dot{\boldsymbol{\omega}} \times \mathbf{r}_i & \\ +\boldsymbol{\omega} \times (\mathbf{u} + \boldsymbol{\omega} \times \mathbf{r}_i) & \\ +\dot{\mathbf{u}}_i + 2\boldsymbol{\omega} \times \mathbf{u}_i] & \\ +\dot{m}_i(\mathbf{u} + \mathbf{u}_i + \boldsymbol{\omega} \times \mathbf{r}_i) &= \mathbf{f}_i + m_i\mathbf{g} \end{aligned} \qquad (3)$$

where the expressions are;

m, m_i,	ship mass, lumped mass,
$\mathbf{I}$,	ship rotational inertia matrix,
$\mathbf{u}, \mathbf{u}_i$,	ship-, lumped mass velocity,
$\boldsymbol{\omega}$	ship angular velocity,
$\mathbf{r}_i$,	lumped mass location in ship coordinates,
$\mathbf{f}, \mathbf{m}$,	force-, moment vector,
$\mathbf{g}$,	gravitational acceleration vector.

Sub-index *i* denotes lumped mass and *ext* external force. Equations (1, 2) and equation (3) are coupled through the interacting force $\mathbf{f}_i$.

The location of the lumped mass at each time step for given roll angle is calculated from the tank geometry and the water volume. Floodwater free surface is assumed to remain horizontal. This allows the calculation of the lumped mass location from the tank tables. Now that the location of the lumped mass is known its impact to the ship motions can be taken into account by combining the lumped mass equations of motion with the ship equations of motion. This yields the following set of equations (4) written in matrix form in six degrees of freedom.

$$
\begin{aligned}
&\left(\begin{bmatrix} mI_{3\times 3} & 0 \\ 0 & \mathbf{I} \end{bmatrix}\right. \\
&\left. +m_i \begin{bmatrix} I_{3\times 3} & -\mathbf{S}(\mathbf{r}_i) \\ \mathbf{S}(\mathbf{r}_i) & -\mathbf{S}(\mathbf{r}_i)\mathbf{S}(\mathbf{r}_i) \end{bmatrix}\right) \begin{Bmatrix} \dot{\mathbf{u}} \\ \dot{\boldsymbol{\omega}} \end{Bmatrix} && \text{(i)} \\
&\qquad + \begin{Bmatrix} m\boldsymbol{\omega} \times \mathbf{u} \\ \boldsymbol{\omega} \times \mathbf{I}\boldsymbol{\omega} \end{Bmatrix} \\
&+ \begin{bmatrix} I_{3\times 3} \\ \mathbf{S}(\mathbf{r}_i) \end{bmatrix} \{ m_i \boldsymbol{\omega} \times (\mathbf{u} + \boldsymbol{\omega} \times \mathbf{r}_i) && \text{(ii)} \\
&\qquad +m_i \dot{\mathbf{u}}_i && \text{(iii)} \\
&\qquad +2m_i(\boldsymbol{\omega} \times \mathbf{u}_i) && \text{(iv)} \\
&\qquad +\dot{m}_i(\mathbf{u} + \mathbf{u}_i + \boldsymbol{\omega} \times \mathbf{r}_i)\} && \text{(v)} \\
&\qquad\qquad = \begin{Bmatrix} \mathbf{f}_{ext} \\ \mathbf{m}_{ext} \end{Bmatrix} + \begin{Bmatrix} m\mathbf{g} \\ 0 \end{Bmatrix} \\
&\qquad\qquad + \begin{bmatrix} I_{3\times 3} \\ \mathbf{S}(\mathbf{r}_i) \end{bmatrix} m_i \mathbf{g} && \text{(vi)} \qquad (4)
\end{aligned}
$$

where the $I_{3\times3}$ is an identity matrix of size 3×3 and the vector cross product with $\mathbf{r}_i$ is operated by matrix $\mathbf{S}(\mathbf{r}_i)$ defined as

$$
\mathbf{r}_i = \begin{Bmatrix} x_i \\ y_i \\ z_i \end{Bmatrix}, \quad \mathbf{S}(\mathbf{r}_i) = \begin{bmatrix} 0 & -z_i & y_i \\ z_i & 0 & -x_i \\ -y_i & x_i & 0 \end{bmatrix}. \qquad (5)
$$

The effect of the lumped mass consists of an added inertia to the generalized mass matrix of the ship (i), of a force related to the lumped mass centripetal acceleration (ii), force related to the acceleration of the lumped mass with respect to the ship (iii), Coriolis force (iv), lumped mass rate of change (v) and of a gravitational force due to lumped mass weight (vi).
The terms currently implemented to calculation method are lumped mass inertia (i), lumped mass centripetal acceleration (ii) and lumped mass gravitational force (vi).

4 CASE STUDY

4.1 Studied ship

A passenger ship, cruise vessel, designed by Meyer Werft designated as Concept ship B is used for flooding simulations. The details of the ship are given in the Floodstand deliverable D1.1b *(Luhmann 2009)*. The compartment arrangements are shown below in Figure 1 for decks 1 and 2 where the flooding extends.

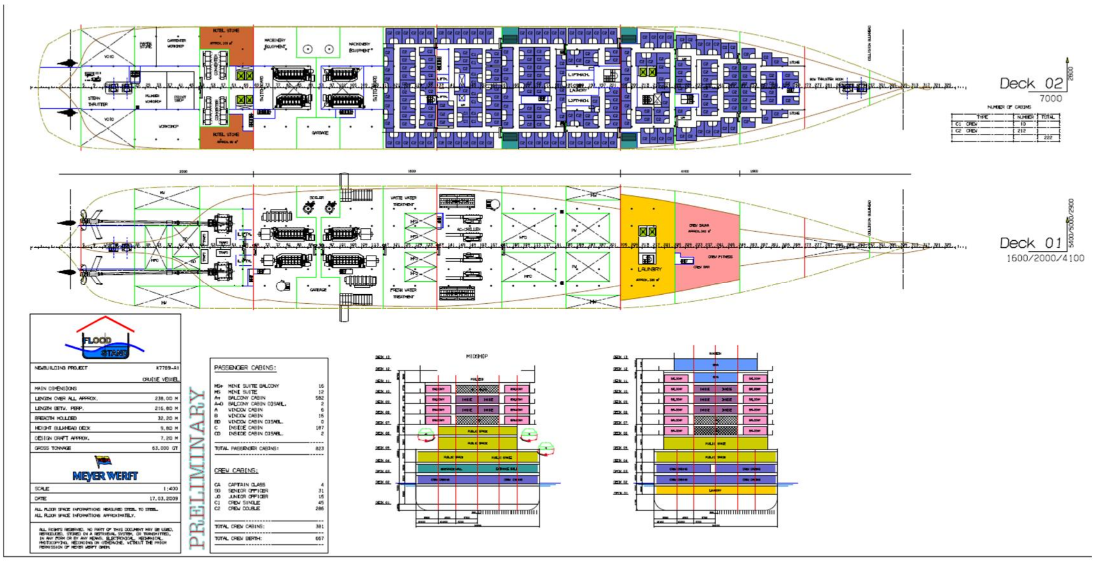

Figure 1. Compartment arrangements of the concept ship B at decks 1 and 2.

The main dimensions of the intact ship are listed below in the Table 1.

Table 1. Concept ship B, main dimensions.

Loa	238.00	m
Lpp	216.80	m
B	32.20	m
H bulkhead deck	9.80	m
T	7.20	m
displacement	35 367	t
deadweight	8 900	t
GT	63 000	

The exact values of the radius of gyration are not known at this concept stage so the standard values used normally in the seakeeping tests are applied.

Table 2. Concept ship B, properties.

GM_0	2.62	m
ZG	15.185	m
k_{xx} (0.42 B)	13.524	m
k_{yy} (0.26 Lpp)	56.368	m
k_{zz} (0.26 Lpp)	56.368	m
T_ϕ natural roll freq.	18.3224	s
ξ roll damping ratio	0.0144	

4.2 Damage case 1.

The damage opening of the hull is located at the portside, aft from the midship. The outer shell damage extends over two compartments. The forward flooded compartment is engine room (R71). The flooded compartment further back is modelled as two rooms; boiler room (R61P) and a garbage room (R61S), see Table 3 and Figure 2. The cross-flooding between the boiler- and garbage rooms is arranged through transverse corridor. This is modelled as a single opening with height of 2 m. Outer shell damage openings are modelled as point openings with given area and discharge coefficient *Cd*. Damage opening areas and discharge coefficients are given below in Table 4.

Table 3. Flooded rooms at damage case 1.

tag	function	permeability	net volume(m^3)
1. R71	Engine room	0.85	2725.0
2. R61P	Boiler room	0.85	822.9
3. R61S	Garbage room	0.85	822.9

Table 4. Damage case 1. Openings.

location between		area(m^2)	Cd
sea	R61P	15.0	0.6
sea	R71	2.0	0.6
R61P	R61S	2.0	0.6

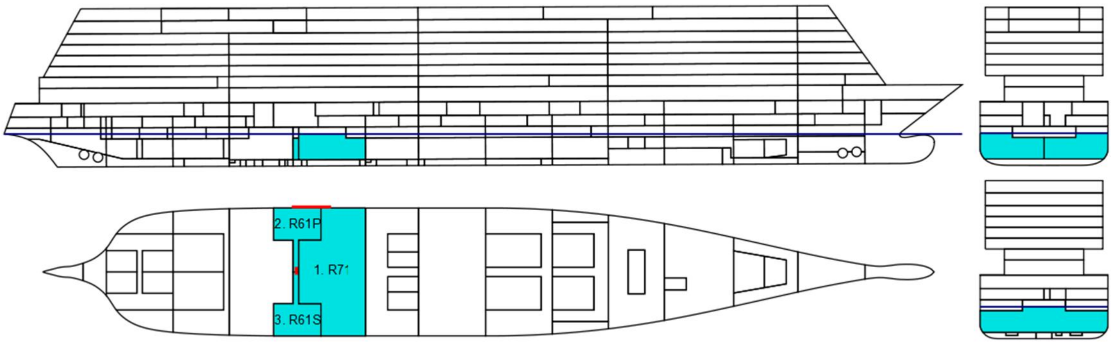

Figure 2. Damage case 1. Flooded rooms. Damage opening on the portside and the opening between the rooms 2. (R61P) and 3. (R61S) are marked with red on the picture.

4.3 Damage case 2.

In the second damage case the opening extended over three contiguous compartments. The purpose of the second damage case was to model extensive flooding and an asymmetric final flooded condition with notable steady heeling angle. For this purpose the engine room compartment (R71) was divided longitudinally into two rooms R71P and R71S by placing a longitudinal bulkhead with an opening in the middle. Moreover, the compartment in front of the engine room was divided also by a longitudinal bulkhead and assuming this bulkhead fully watertight. This three compartment damage is modelled as five flooded rooms. Definitions of the flooded rooms are listed in the Table 5 and the locations can be viewed at Figure 3.

Table 5. Flooded rooms at damage case 2.

tag	function	permeability	net volume(m^3)
1. R61P	Boiler room	0.85	822.9
2. R61S	Garbage room	0.85	822.9
3. R71P	Engine room portside	0.85	1362.5
4. R71S	Engine room starboard	0.85	1362.5
5. R81P	Waste water treatment	0.85	791.5

The portside rooms (R61P, R71P and R81P) had a damage opening to the sea. The total area of the damage opening is approximately one quarter of the size of the damage opening at case 1. Cross-flooding through the corridor between the rooms R61P and R61S has the same area as in the previous damage case, except that it is first closed and leaking and collapses at the pressure equal to the 2.0 meter water column height. The opening between the R71P and R71S is quite small with 0.5 m^2 area. This opening is also closed and leaking before collapsing at the 0.5 meter water column equivalent pressure. Some rather high collapsing pressure heights are used to ensure further asymmetry during the flooding process. Therefore, the data from Tasks 2.1 and 2.2 is not used. It should be noted that this is an unrealistic situation that has been created only for testing purposes. Definitions of the openings are listed in the Table 6.

Table 6. Damage case 2. Openings.

location between		leaking area(m2)	area(m^2)	Cd	collapse pressure
sea	R61P	-	3.0	0.6	-
sea	R71P	-	1.0	0.6	-
sea	R81P	-	0.5	0.6	-
R61P	R61S	0.02	2.0	0.6	2.0 m water column
R71P	R71S	0.05	0.5	0.6	0.5 m water column

Flooded rooms and the openings are shown in Figure 3. The final equilibrium stage of the flooding in the calm water condition at the cross sections (A,B,C) are shown below in Figure 3.

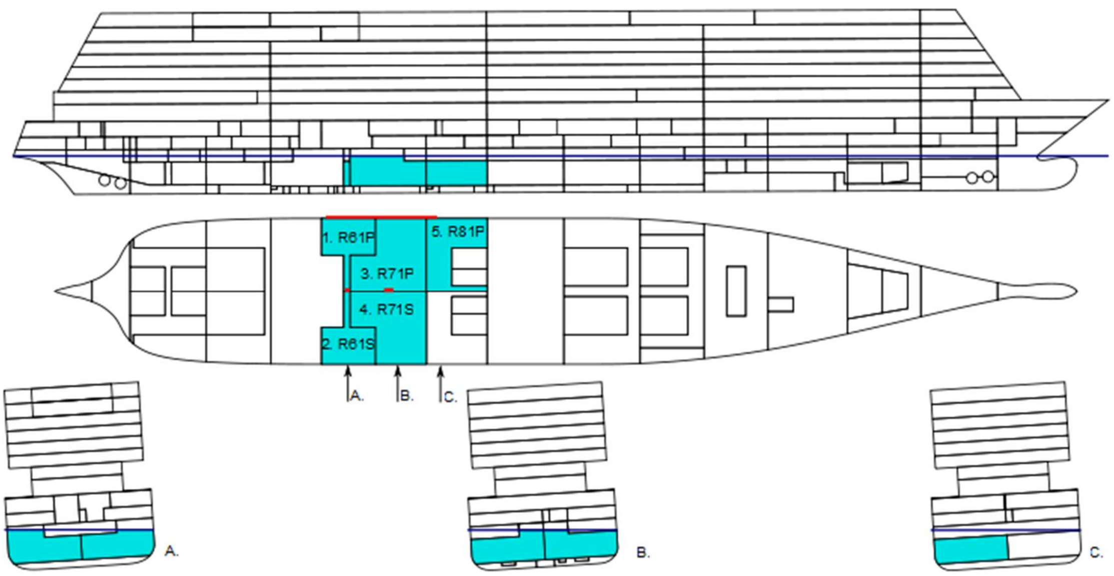

Figure 3. Damage case 2. Openings and flooded rooms. Sections at longitudinal positions A,B and C are shown.

5 RESULTS

5.1 Simulated cases

The conceivable operational area of the concept cruise ship could have wave conditions ranging from 2.5 meters to at least 6.5 meters though the cruise vessels usually try to avoid harsh sea conditions in normal operation in order to guarantee passenger comfort. Beam seas are regarded as the worst wave direction for a stationary flooding ship. Ship motions were simulated at four different sea states; calm seas and at three irregular sea states. The response of the intact ship in starboard beam seas is calculated in order to have a reference to the impact of the flood water to the roll motion in damage condition. Irregular waves of JONSWAP spectrum are generated. Heights of the waves are increased during the first 50 seconds of the simulation by a ramp function to avoid the transient wave response motion of the ship. Significant wave heights *Hs* of the spectrums were varied from 2.5 meters up to 6.5 meters. The peak period *Tp* of the spectrum was defined such that the wave steepness at peak period for the significant wave height is Hs/λ=0.04. The wave time histories for the realization of the irregular JONSWAP spectrum are shown in the figures. Equally the simulated roll time histories are shown. Spectrum of the wave realization and the simulated roll was calculated. The simulated roll angle in the damage cases was smoothened with calculation of the moving average over a period longer than the ship natural roll period.

Table 7. Matrix of simulated cases.

	wave		intact	damage case	
	Hs(m)	Tp(s)	0.	1.	2.
0.	0	-	-	x	x
1.	2.5	6.33	x	x	x
2.	4.0	8.00	x	x	x
3.	6.5	10.20	x	x	x

The mean roll period $T_{1\phi}$ was calculated from the spectrum of the roll motion for the frequencies higher than 0.18 rad/s. For the intact ship the mean roll frequencies are smaller but close to the natural roll frequency due to the wave spectrum. At first damage case the mean roll frequencies are higher due to the slightly improved stability when the flooded water has reached the bottom compartments. At the second damage case in wave conditions the frequencies are the smallest. The residual stability of the ship at the second case is slightly poorer due to the inserted longitudinal bulkheads.

Table 8. Mean roll period $T_{1\phi}$ calculated from the spectrum.

	wave		intact	damage case	
	Hs(m)	Tp(s)	0.	1.	2.
0.	0	-	-	20.59	18.99
1.	2.5	6.33	17.19	19.01	14.44
2.	4.0	8.00	17.52	19.31	15.03
3.	6.5	10.20	17.79	18.31	15.37

5.2 Intact ship in waves

Wave and roll time histories of the simulation as well as their spectra for the studied sea states are shown in sub-chapters 5.2.1 – 5.2.3.

5.2.1 Intact ship, sea state Hs = 2.5 m

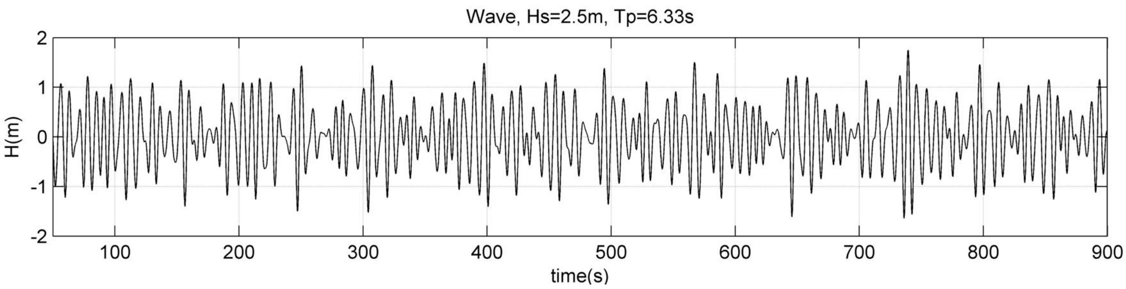

Figure 4

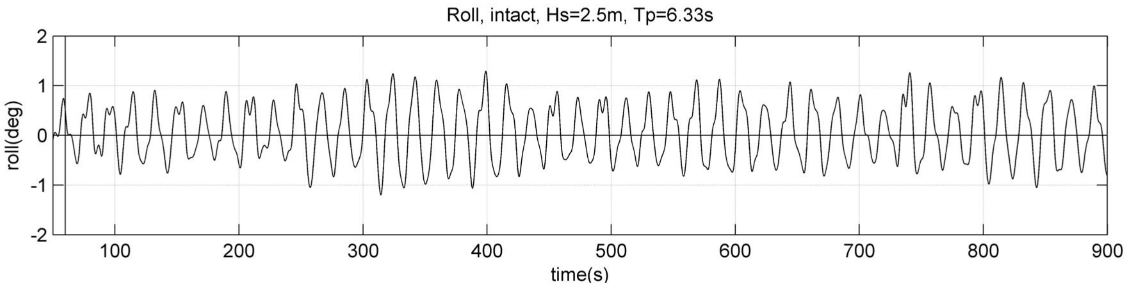

Figure 5

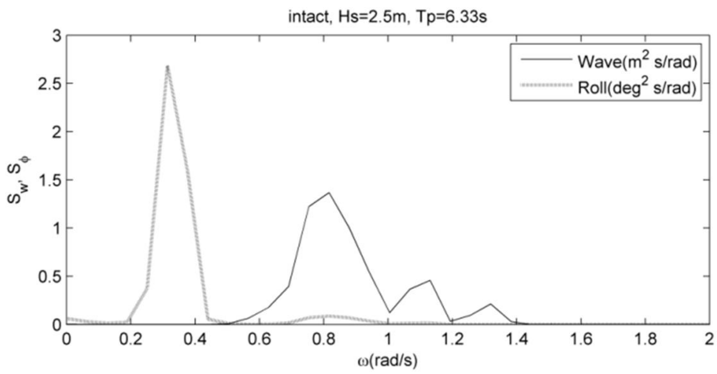

Figure 6

5.2.2 Intact ship, wave case Hs = 4.0 m

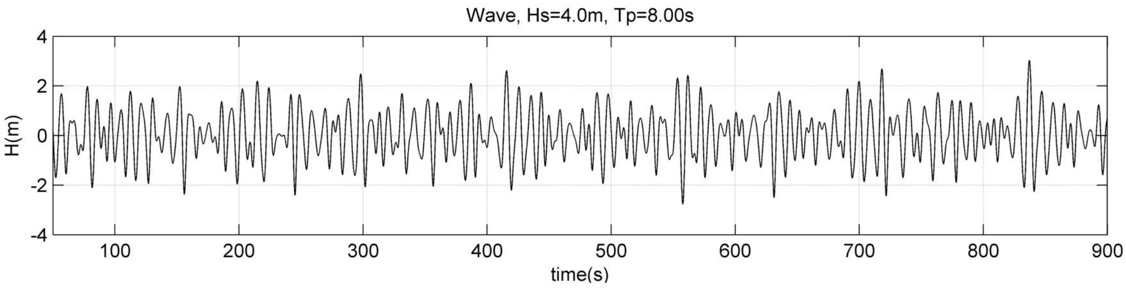

Figure 7

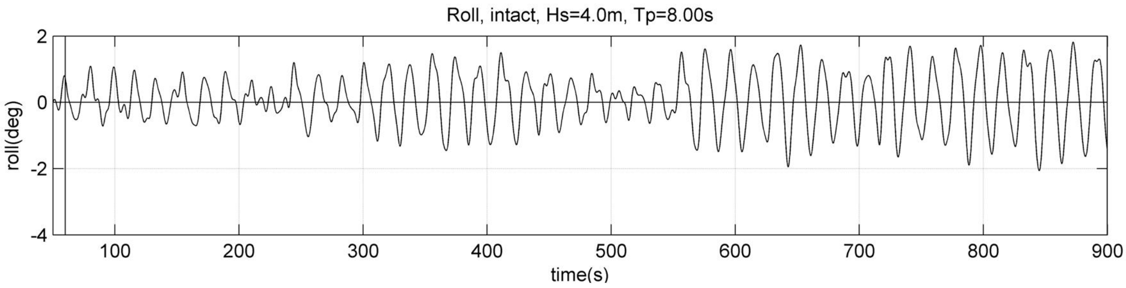

Figure 8

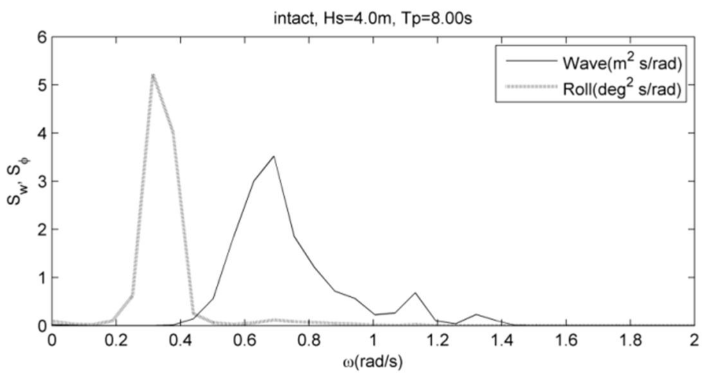

Figure 9

5.2.3 Intact ship, wave case Hs = 6.5 m

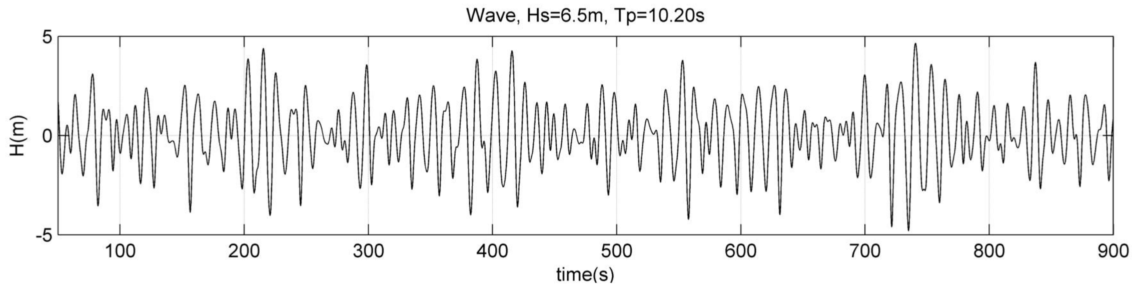

Figure 10

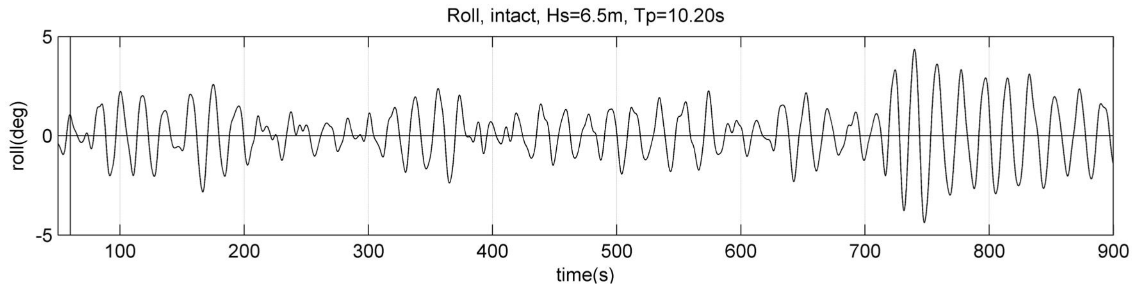

Figure 11

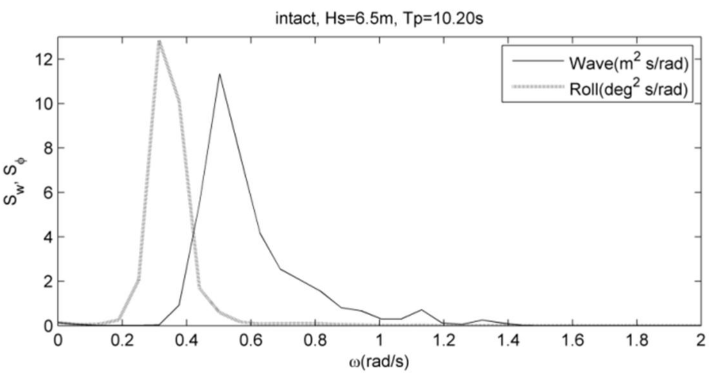

Figure 12

5.3 Damage case 1.

Damage is introduced to the ship at simulation time 60 seconds. Flooding reaches all three rooms immediately after the damage. Compartment R61P (Boiler room) on the portside fills up within 15 seconds from the damage. Flow rate to the room R71 (engine room) is slower due to smaller breach. Room R61S (garbage room) on the starboard is flooded through the cross flooding duct between the rooms R61P and R61S. During the first 15 seconds from the damage the flooding is highly asymmetric, Figure 13. This causes the ship to heel four degrees to the port side on the quasi-static simulation and nearly seven degrees maximum roll angle is observed at the dynamic simulation, Figure 14.
Two minutes after the damage flood water volumes in the rooms R61S and R61P are even and in the quasi-static simulation heel angle become zero. Flooding to the symmetrical room R71 continues but it does not cause any heel angle at this stage.

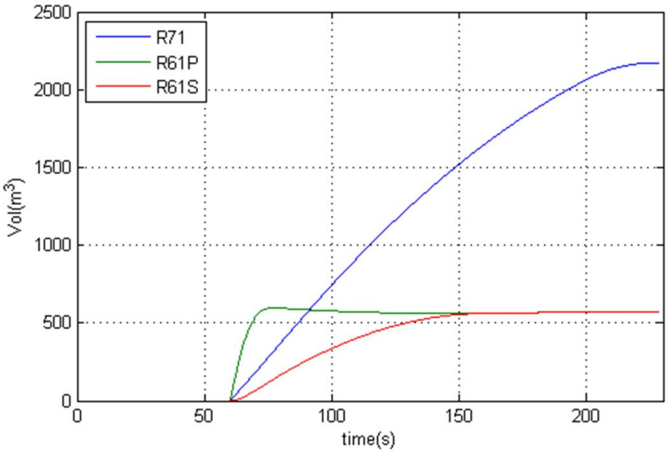

Figure 13. Floodwater volumes in the rooms. Result of the quasi-static simulation.

5.3.1 Damage case 1, sea state calm

At the simulation with the dynamic model the abrupt flooding to the portside room R61P causes transient roll angle, which is seen to decay around the heel angle simulated by the quasi-static model. A moving average over a period longer than the ship natural roll period T_ϕ was calculated of the simulated roll angle result. Moving average smoothens out the transient roll from the dynamic simulation result. Quasi-static heel angle and moving average of the dynamic simulation correspond quite closely, Figure 14.

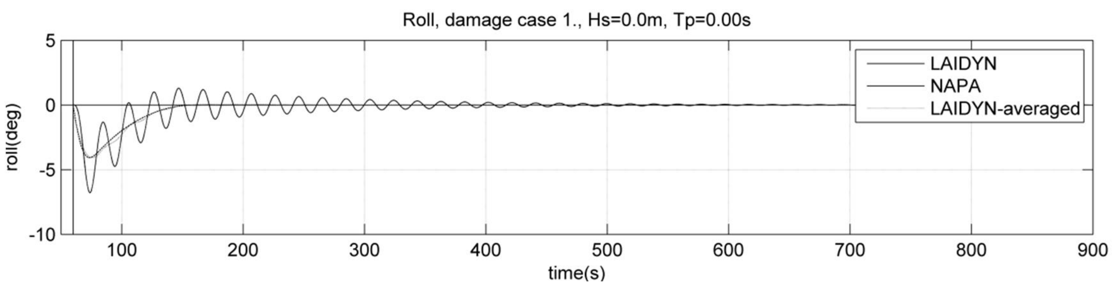

Figure 14. Roll angle of the damage case 1 at the calm sea state.

Trim angle increases with the increasing total amount of the floodwater. On the whole, the trim angle is small, under 0.25 degrees. Both the quasi-static and the dynamic simulation predict similar trim angle the difference between them is very small. No large oscillations are seen on the trim angle of the dynamic simulation, Figure 15.

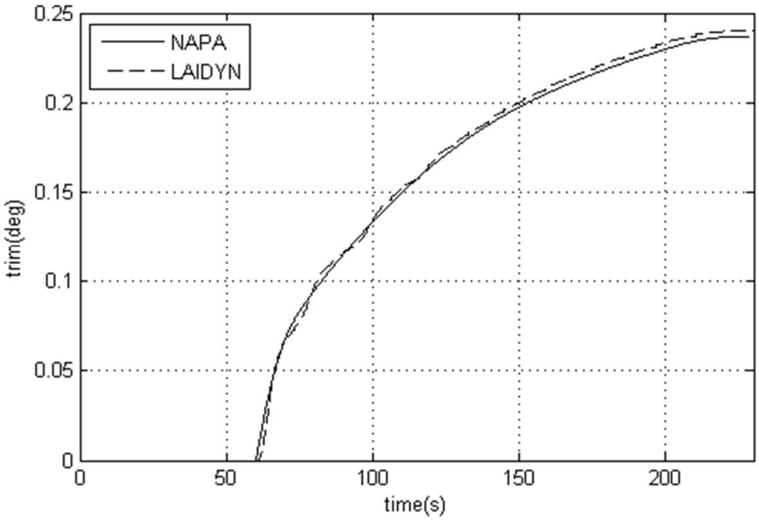

Figure 15. Trim angle of the damage case 1 at the calm sea state.

The spectrum of the roll angle is shown in the Figure 16. The mean period of the roll angle is calculated from the spectrum, where the frequencies lower than 0.18 rad/s are eliminated, $T_{1\phi}$=20.6 s.

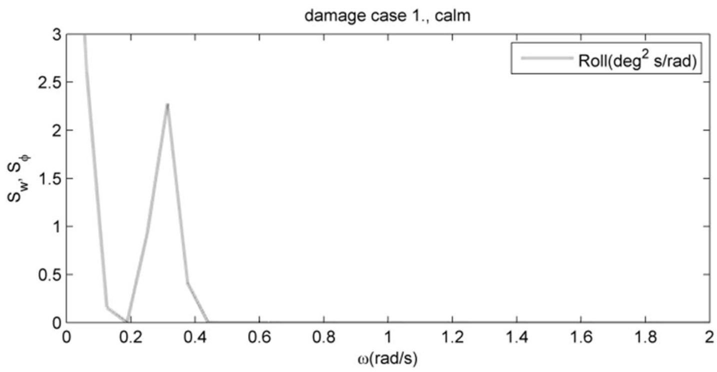

Figure 16. Damage case 1. Power spectrum of the roll angle.

Time histories of the wave height and roll angle as well as the power spectra of the roll angle for the other sea states (Hs=2.5 m, 4.0 m and 6.5 m) are presented in the following sub-chapters 5.3.2 – 5.3.4.

5.3.2 Damage case 1, sea state Hs = 2.5 m

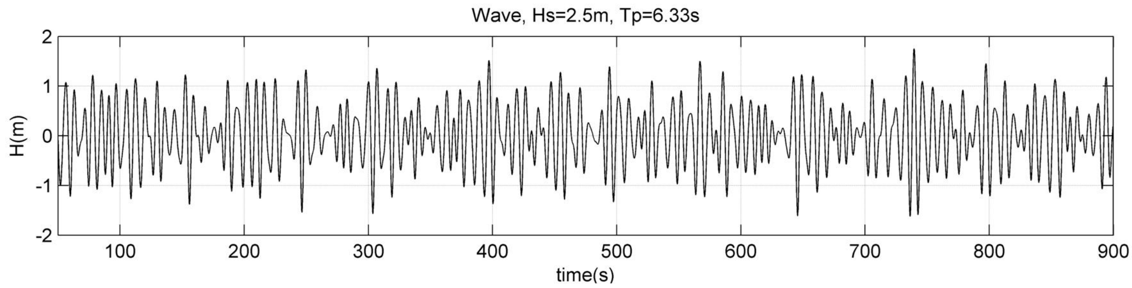

Figure 17

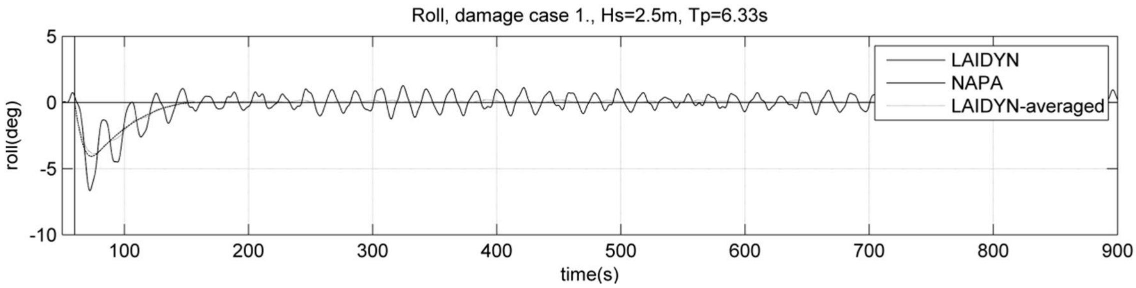

Figure 18

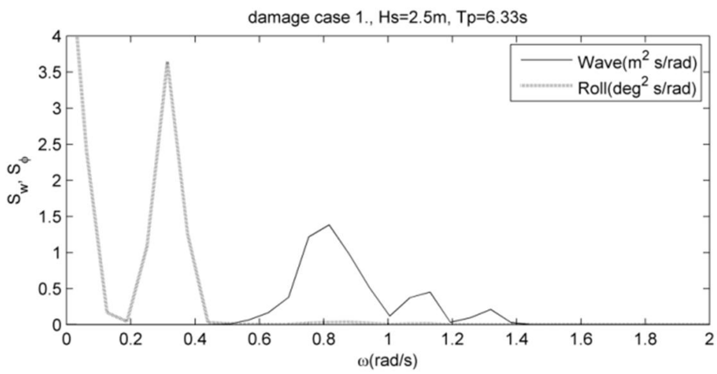

Figure 19

5.3.3 Damage case 1, sea state Hs = 4.0 m

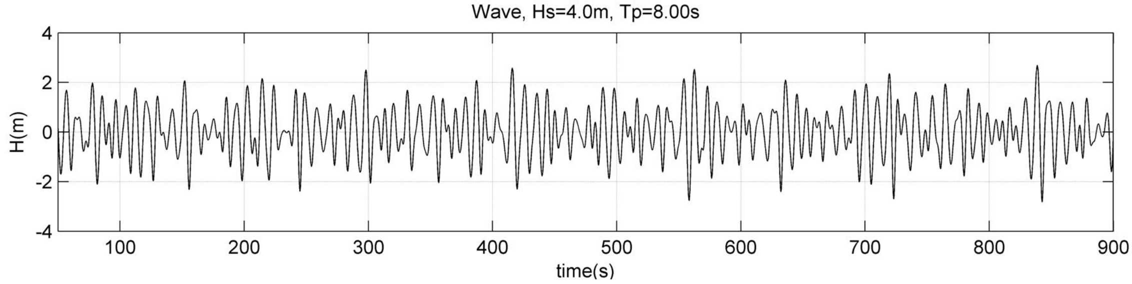

Figure 20

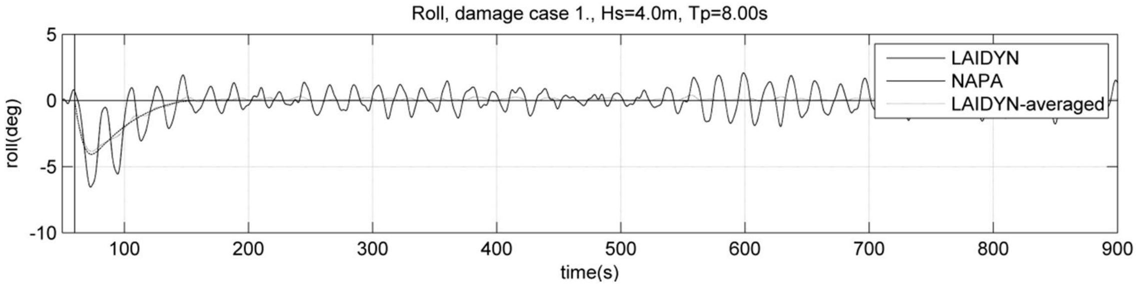

Figure 21

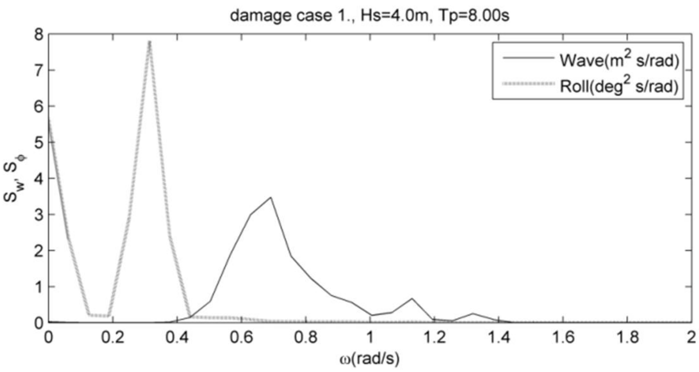

Figure 22

5.3.4 Damage case 1, sea state Hs = 6.5 m

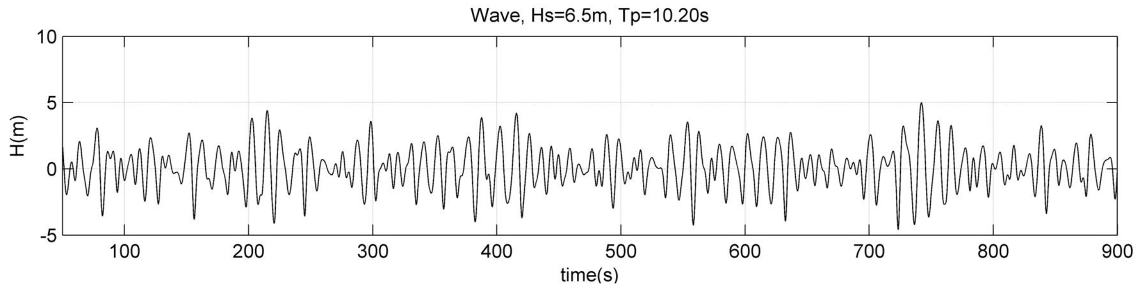

Figure 23

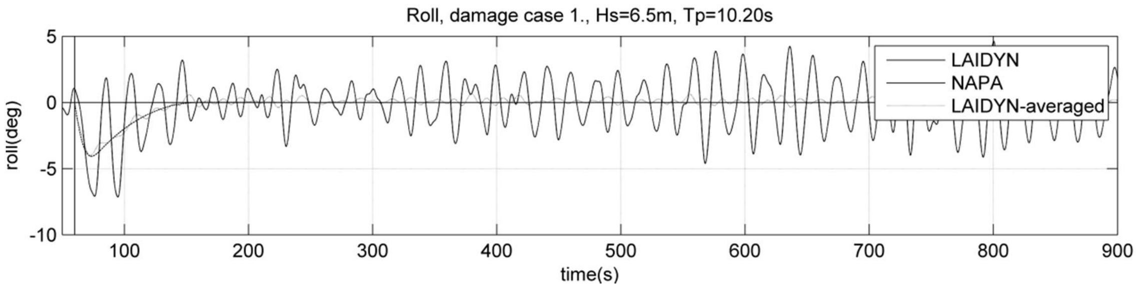

Figure 24

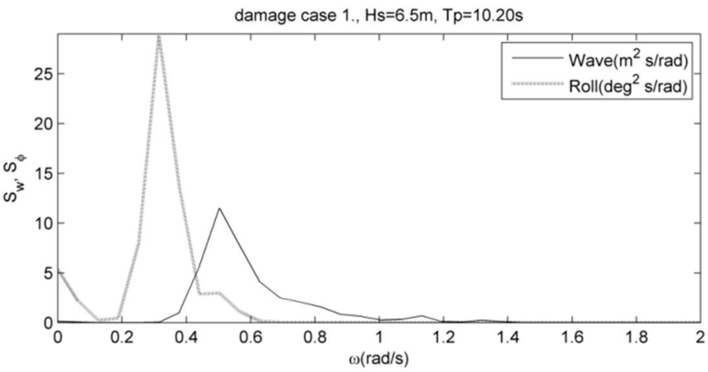

Figure 25

5.4 Damage case 2. Results

First the water starts to flood in the three rooms on the portside; R61P, R71P and R81P. Only 0.7 seconds after the damage, the leaking opening between the rooms R61P and R61S collapses and room R61S starts to flood. Flooding to the starboard of the engine room starts 155.7 seconds after damage. After 274.0 seconds from the damage the room R81P is completely full. By this time all the flooded rooms are full or nearly full except for the R71S.

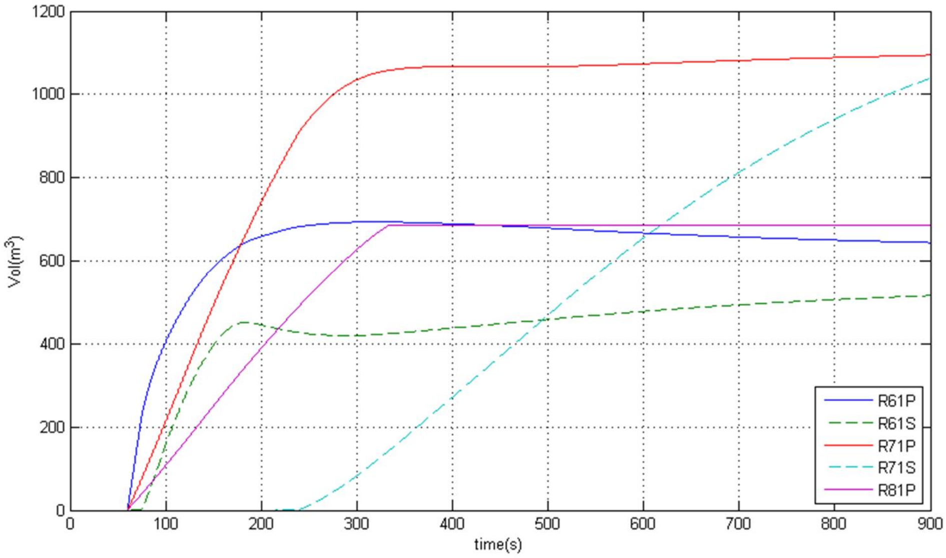

Figure 26. Damage case 2. Floodwater volumes result of the quasi-static simulation at calm water.

5.4.1 Damage case 2, sea state calm

In this damage case the flooding is asymmetric, but it is not that fast as in the first damage case. The transient roll angle is relatively small compared to the slowly changing overall heel angle. Maximum angle is achieved slowly after the damage and it is not caused by the transient roll. Eventually the heel angle starts to decrease as the floodwater amount on the starboard side rooms increases. Final equilibrium angle of the heel is close to four degrees. At calm sea state the quasi-static NAPA- and dynamic LAIDYN-simulation predict closely the same roll angle, dynamic simulation roll angle being slightly higher. The difference between the predicted roll angle by NAPA and LAIDYN decreases towards the end of the simulation.

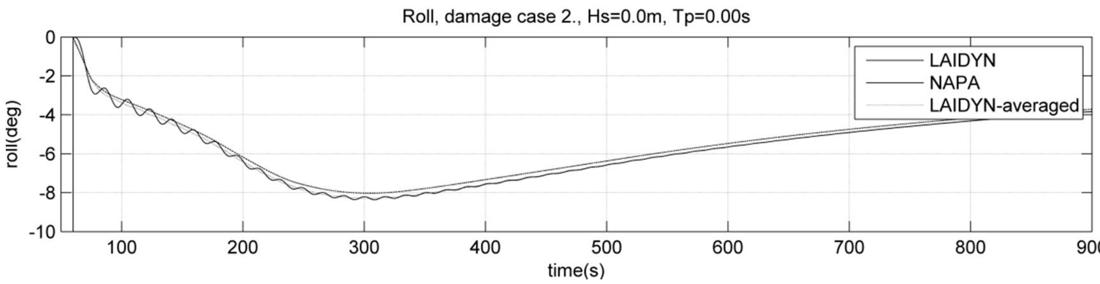

Figure 27. Damage case 2. Roll angle at calm sea state.

The trim angle increases monotonically with the increasing amount of the floodwater as in the previous damage case. The trim angles predicted by the NAPA and LAIDYN simulations are nearly equal. No transient pitch motions are observed on the simulation result, Figure 28.

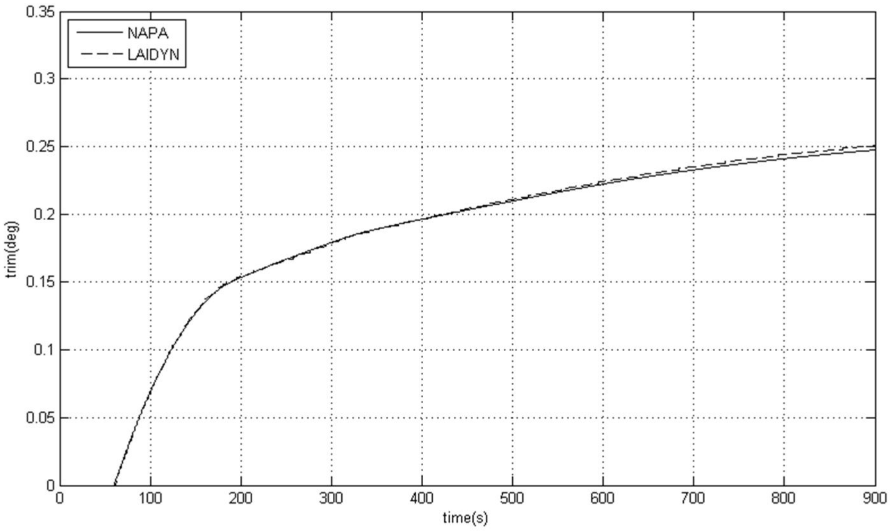

Figure 28. Damage case 2. Trim angle result at calm water. Quasi-static simulation with NAPA and dynamic simulation with LAIDYN.

The power spectrum of the dynamic roll motion is shown at the . The mean roll period over the whole simulation time calculated from the spectrum where the frequencies below 0.18 rad/s are eliminated is 19.0 seconds.

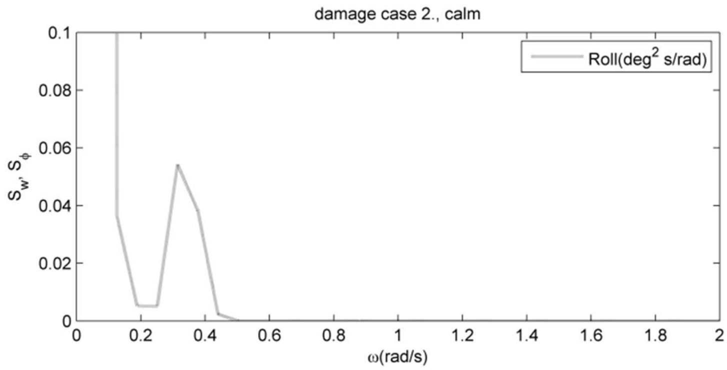

Figure 29. Damage case 2. Power spectrum of the roll motion.

Time histories of the wave height and roll angle as well as the power spectra of the roll angle for the other sea states (Hs=2.5 m, 4.0 m and 6.5 m) in damage case 2. are presented in the following sub-chapters 5.4.2 – 5.4.4.

5.4.2 Damage case 2, sea state Hs = 2.5 m

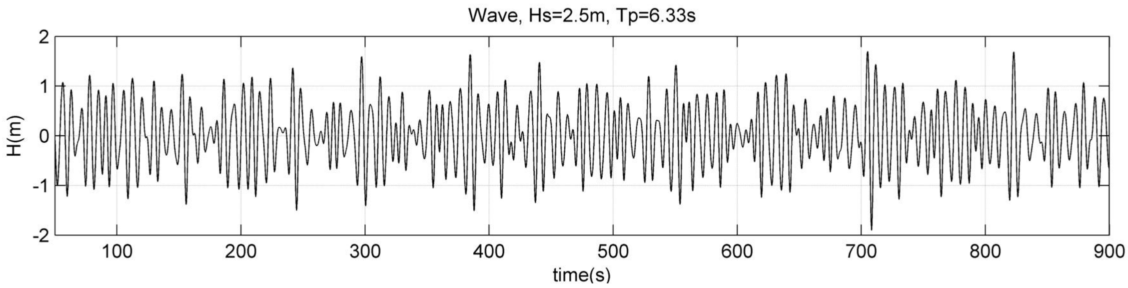

Figure 30

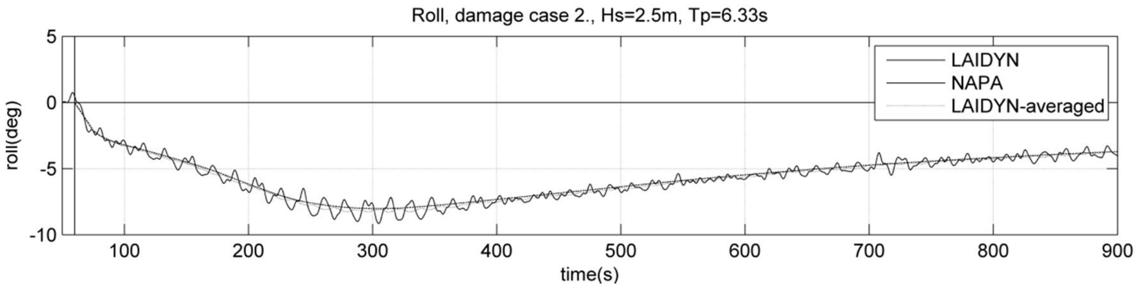

Figure 31

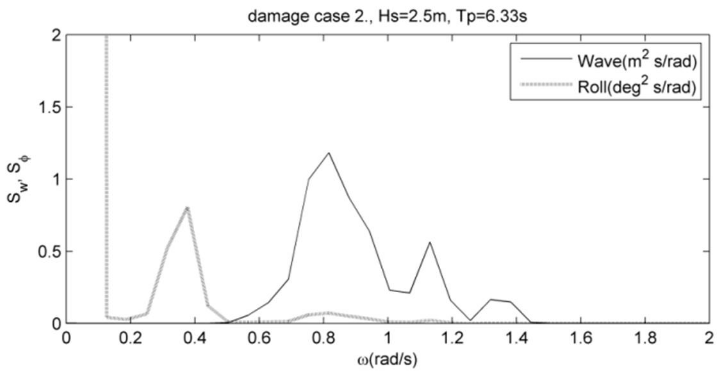

Figure 32

5.4.3 Damage case 2, sea state Hs = 4.0 m

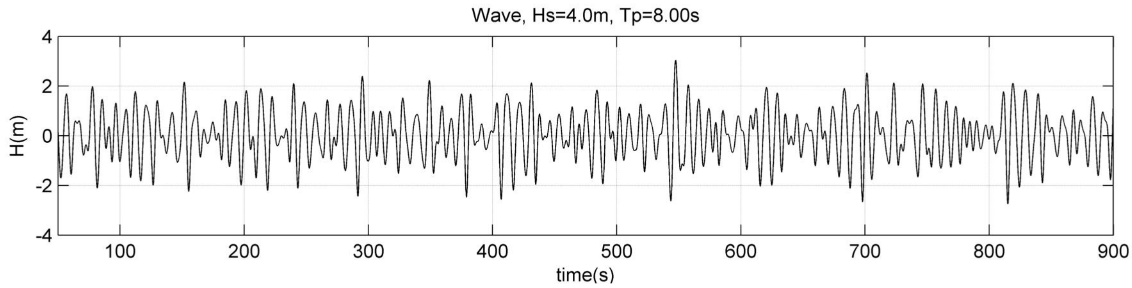

Figure 33

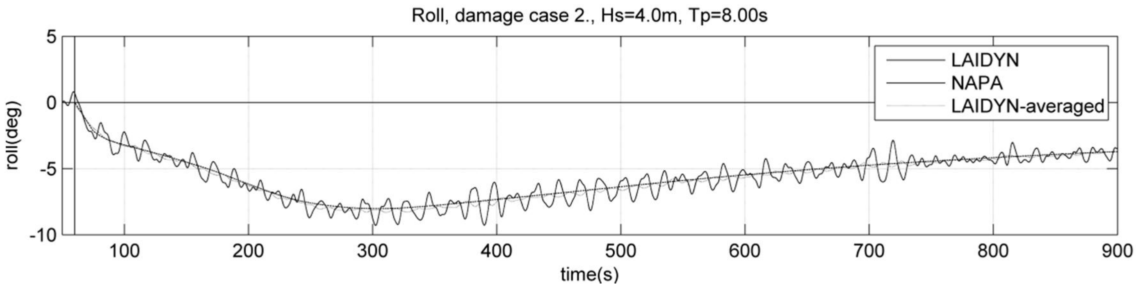

Figure 34

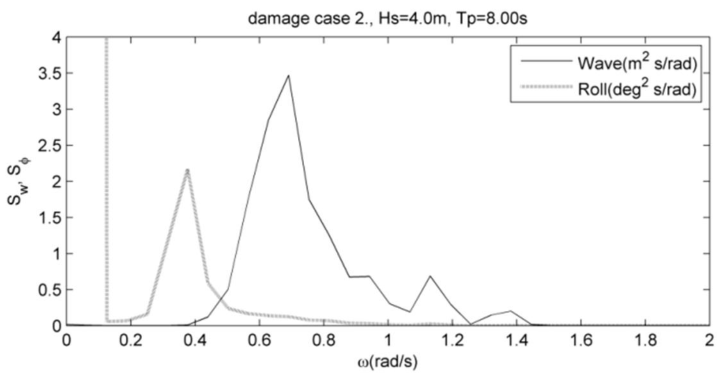

Figure 35

5.4.4 Damage case 2, sea state Hs = 6.5 m

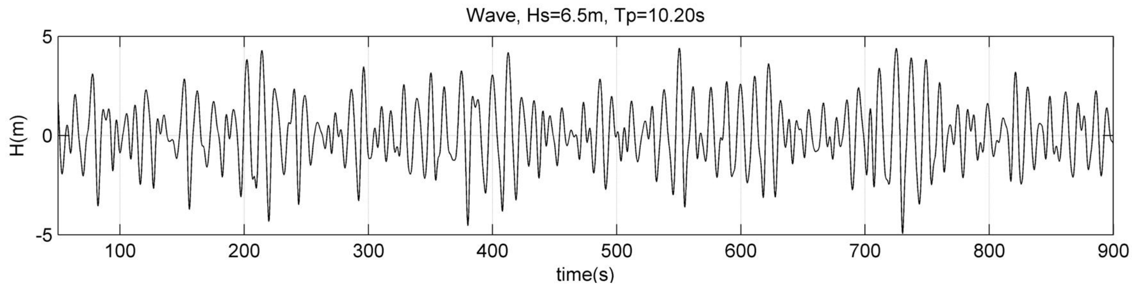

Figure 36

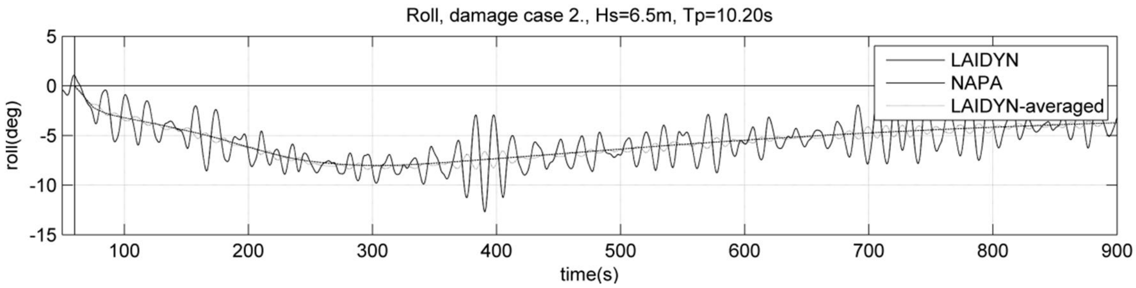

Figure 37

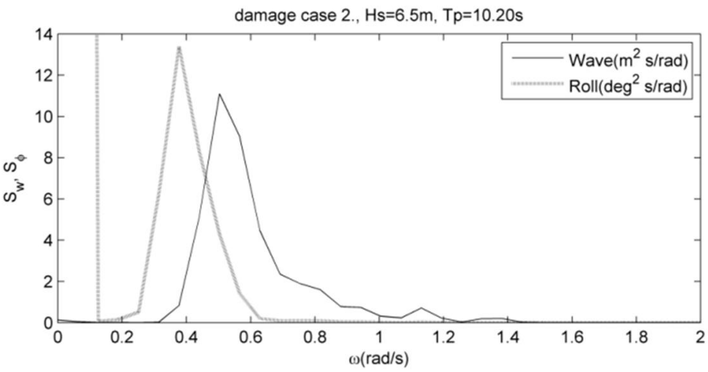

Figure 38

6 CONCLUSIONS

Transient effect is more important when the flooding through the outer shell opening is fast. This can be seen in the first damage case where the dynamic roll angle is almost twofold when compared to the maximum heel angle obtained with the quasi-static simulation. In the second damage case the overall flooding is more severe and causes a higher heel angle. Transient roll angle is smaller in this case than the static heel angle.

Simulations of the ship motions in the studied waves show that the ship rolls around the quasi-static heel angle calculated at the calm water condition. Due to the limitations of the model used in this study the amounts of the flood water were not affected by the roll motions. They were taken as the input from the quasi-static simulations.

The results of this study in the first damage case show that the damage stability of the ship is hardly deteriorated. Cross flooding duct allows the water to disperse laterally and the asymmetric flooding stage is rather short. Eventually, as the rooms fill up, the lateral movement of the flood water becomes very limited. Furthermore the centre of gravity of the floodwater in these rooms is located low in the ship which improves the stability by lowering the total centre of gravity of the ship and the floodwater.

In the second damage case the damage stability of the ship was artificially decreased by altering the divisions of the flooded compartments. In this case larger quasi-static heel angle than in the first case was obtained. In the second damage case the final static position of the ship remains inclined to the portside. Added longitudinal divisions did not allow the floodwater to even up between the adjacent rooms and holds the ship at final heel angle of 3.6 degrees at calm water.

At the damage case in prevailing wave conditions the ship roll angle is induced by both the waves and floodwater. What comes to the prediction of the flooding by the use of the flooding sensors, the motions of the ship induced by the waves must be distinguished from the ones induced by the flooding. The response of the ship motions to the slowly progressive flooding is generally slower than the response to the waves or to fast abrupt flooding. Quasi-static ship position can be distinguished from the overall dynamic response of the ship by calculating the moving average of the predicted dynamic motions. Results show that the moving average calculated over a period about ten percentages longer than the ship natural roll period yields nearly the same heel angle than the quasi-static simulation.

The results presented are obtained with one-directional simulation of the flooding. Dynamic simulations are performed with given floodwater volumes and the dynamic motions do not have any impact to the flooding process as mentioned before. This is a severe limitation to a clearly coupled phenomenon of flooding and ship motions. Furthermore the assumption of the horizontal floodwater surface is another limitation. Floodwater movement in the complex compartment geometries of a cruise vessel depend on the permeability of the flooded rooms and on the shapes of the obstacles inside them. The viscous forces play an important role in the floodwater dynamic movements. The flow is highly damped and the sloshing in such rooms is probably limited to minimum. The simplified method capable to account for the floodwater and ship motions in flooding is to be studied for fast or real time prediction of the damage ship motions and stability.

7 REFERENCES

Luhmann, H. (2009) Concept Ship Design B, FLOODSTAND Deliverable D1.1b, 19 October 2009. http://www.tkk.fi/Units/Ship/Research/FloodStand/Public/Info/Files/deliverable_D1.1b_v03.pdf

de Kat, J. O. (2000). Dynamics of a ship with partially fooded compartment. In Vassalos, D.,Hamamoto, M., Papanikolaou, A., and Molyneux, D., editors, Contemporary Ideas on Ship Stability, pages 249-263. Elsevier Science.

Jasionowski, A. (2001). An Integrated Approach to Damage Ship Survivability Assessment. PhD thesis, University of Strathclyde.

Manderbacka, T., Matusiak, J. and Ruponen, P. (2011). Ship Motions Caused by Time-Varying Extra Mass on Board. In Proceedings of the 12th International Ship Stability Workshop, pages 263-269, Washington D.C. U.S.A.

Matusiak, J. (2003). On the eects of wave amplitude, damping and initial conditions on the parametric roll resonance. In Proceedings of the 8th International Conference on Stability of Ships and Ocean Vehicles, pages 341-347, Madrid, Spain.

Matusiak, J. (2007). On certain types of ship response disclosed by the two-stage approach to ship dynamics. ACME, Archives of Civil and Mechanical Engineering, VII(4):151-166.

Matusiak, J. (2010). On the non-linearities of ship's restoring and the froude-krylov wave load part. In Proceedings of the ITTC Workshop on Seakeeping, Seoul, Korea.

Papanikolaou, A. (2008). Benchmark study on numerical codes for the prediction of damage ship stability in waves. In Proceedings of the 10th International Ship Stability Workshop, Daejeon, Republic of Korea.

Ruponen, P. (2006). Pressure-correction method for simulation of Progressive Flooding and Internal Air Flows. Schiffstechnik - Ship Technology Research, 53(2):63-73.

Ruponen, P. (2007). Progressive flooding of a damaged passenger ship. PhD thesis, Helsinki University of Technology, Ship Laboratory.

Santos, T. A. and Soares, C. G. (2008). Study of damaged ship motions taking into account flood-water dynamics. Journal of Marine Science and Technology, 13(3):291-307.